International Journal of Research in Engineering and Science (IJRES)
ISSN (Online): 2320-9364, ISSN (Print): 2320-9356
www.ijres.org Volume 10 Issue 8 ǁ August 2022 ǁ PP. 497-504

Cascaded Segmentation and Classification System for Computer-Aided Recognition of Cell Quantification

Kiruba T, M.E*(Applied Electronics), Ponjesly College of Engineering, Nagercoil*
Dr.M.R. Geetha, M.E*., Ph.D, Professor and Head, Ponjesly College of Engineering, Nagercoil*

Abstract
White blood cells are automatically counted and categorised in peripheral blood pictures using computer-aided imaging techniques. The suggested method is analysed by comparing the differences among basophils and eosinophils' coloured histograms, sizes, and shapes before carrying out the identification technique due to their dissimilar properties. In light of this, the suggested system is designed on a cascaded system that employs a categorisation of segmentation method. This system is known as a classification-segmentation reversible System (CSRS). A Histogram-based Object to Background Disparity (HOBD) criterion was developed before the CSRS system has been used to choose the best colour planes for the preliminary WBC identification (first segmentation). The 3rd polynomial support vector machine (SVM) technique produced an early classification performance of 95.4 per cent when used to examine the local histogram characteristics of two groups. In order to cater to the particular requirements of each of the two predicted categories, transformation-based segmentation algorithms were then developed in the suggested CSRS approach. The suggested CSRS classification is utilized, in which each class's categorization procedure receives images from a preliminary classifier. The classification results showed that eosinophils and basophils had similarity indices of 97.1 percent and 98.9 percent, correspondingly. Additionally, both classes had average counting accuracy of 98.4 percent. Additionally, a second classification was performed after using the CSRS, resulting in an accuracy improvement of 6.4 per cent over the first classification procedure.
Keywords: *White blood cells; Histogram based detection; Support vector machine; Wavelet transform segmentation thresholding; Classification-Segmentation Reversible System;*

Date of Submission: 14-08-2022 Date of acceptance: 29-08-2022

I. Introduction

Red blood cells (RBCs), white blood cells (WBCs), and platelets are the three foremost blood cell types that circulate in the human body. WBCs are mainly noticeable in peripheral blood circulation. These bone marrow-derived cells play a critical part in safeguarding the body and sustaining the immune system[1]. Lymphocytes, monocytes, Eosinophils, neutrophils, and basophils are the major 5 kinds of WBCs [2]. Eosinophils and basophils both contribute significantly to the body's defence against parasite infections, the management of allergic reactions, and the prevention of blood clotting. Pathologists can assess a person's physical health through the vital blood screening procedure. It allows them to gather crucial data, such as the type, amount, and size of WBCs, helping pathologists identify various diseases, such as leukaemia and other blood disorders. For determining how many cells are present in the blood fluid, a wide range of laboratory procedures are taken into account. WBC difference testing, for illustration, is a common medical procedure for a platelet count. In order to identify potential health issues including infections and blood disorders, the absolute count or relative fraction of each type of leukocyte is calculated based on the WBC count's deviation from the recommended ranges. Traditionally, pathologists have carried out differential blood counting by manual methods like blood smear analysis. WBCs are counted under a microscope, either manually or using an image that has been taken[3]

Inaccurate counting results from both human counting errors and the WBCs are not distributed evenly throughout the smear. Additionally, the space-bandwidth product of the traditional microscopes employed in the manual scanning method limits their utilisation, leading to a trade-off between the resolution of the picture and the optical microscope view. For instance, a high magnification objective lens is necessary for a differential count, which results in an extremely small FoV[4]. Flow cytometry-based technologies are more accurate automated counting approaches, but they are also more expensive and unable to determine the morphology or structure of the cells. Therefore, automated image processing technologies provide a sufficient solution in both identification and quantification of microscopic investigation..

Since accurate segmentation is a prerequisite for extracting features, categorization, and cell counting, it is widely recognised as a key step in microscopic image analysis. Since each type of WBC has a unique cell

shape, several segmentation techniques have been developed in the literature[5]. The microscopic imaging properties of the WBCs influence each of these techniques. Typically, WBCs have a distinguishable lilac cytoplasm around a dark-violet nucleus. However, the segmentation and detection processes are made more difficult by the fact that WBCs have a variety of sizes, edges, and shapes in addition to having or not having granules in their cytoplasm. For instance, although eosinophils and basophils are both granulocytic kinds, they differ in appearance. Granules in eosinophils are big and red-orange. The basophils have an irregular shape, dark/large granules, and are smaller than eosinophils in size [6]. WBCs may coexist along Erythrocytes and platelets in the same microscopic examination, making it challenging for computerized cell counters to identify them from the underlying plasma. The feature extraction is further complicated by the fact that, in addition to clumped clusters of overlapping cells, the contrast between the cell contour and its backdrop varies depending on the image-capturing conditions due to illumination irregularities. The document is structured in the manner described below. In Section 3, the proposed system methodology is presented as a general framework for a Computer aided design and tallying system of the two major types of periphery plasma smear images. Following that, Section 4 provides and explains the findings of the suggested method for identifying and counting basophils and eosinophils. The conclusions are noted in Section 5.

II. Related Works

Circulating tumour cells generated by primary and recurrent malignancies are uncommon because they are combined with blood and its components, which makes it difficult to isolate and characterise them. The biology of metastases can be understood in part because of CTCs, which also act as a biomarker to track the non-invasive evolution of tumour genotypes throughout therapy and disease development. A wide range of clinical applications, including early disease detection and the identification of biomarkers to predict treatment responses and disease progression, will be made possible by technological advancements that produce purer CTC populations amenable to better cellular and molecular characterization. However, more advanced analytical techniques will be needed to address CTCs' features [7].

Rare circulating tumour cells (CTCs) have the potential to further our knowledge of cancer metastasis and improve the treatment of cancer patients. In this technique, we outline the steps for isolating rare CTCs from blood samples utilising microfluidic CTC-I Chip technology, which is independent of tumour antigens. The CTC-I Chip sorts up to 107 cells/s using deterministic lateral displacement, inertial focusing, and magnetophoresis. They obtain 3.8-log depletion of white blood cells and a 97 per cent yield of rare cells with a sample processing rate of 8 ml of whole blood/h employing two-stage magnetophoresis and depletion antibodies against leukocytes. Standard cytopathological and RNA-based characterisation techniques are compatible with the CTC-iChip. This protocol outlines the creation, assembling, and processing of the blood sample, system configuration, and CTC isolation procedures. 8 cc of blood must be sorted in 2 hours, comprising setup time, and chip manufacture take 2 to 5 days[1].

When examined through magnification, the distinct counts and examination of lymphocytes can reveal important details about a patient's condition. The three main types of blood cells are platelets, leukocytes, and erythrocytes. RBC, WBC, and platelet counts can be obtained via computerized blood cell analysers, however since the existence of aberrant cells may alter the cells counts, this should be verified manually. In order to quantify and categorise cells, a good clinical decision support system has always been required. There aren't many documented instances of automated systems that can analyse and categorise blood cells. This study suggests using computer-aided systems to automate the detection and identification of WBCs and RBCs from blood smear images. These systems replicate a human visual inspection. With an average accuracy value of 99.2 per cent for WBCs and 98 per cent for RBCs, the suggested method outperforms the state-of-the-art and has been evaluated on public datasets of blood cell pictures. There aren't many documented instances of automated systems that can analyse and categorise blood cells [8].

Blood-borne leukocytes are all in charge of providing defence against diseases. Pathologists use a process known as a differentiated platelet count to detect and quantify the many leukocyte subtypes present in the blood to help diagnose disease. This approach calls for the analyzers to undertake a microscopic review, which takes time and it may result in outcomes that are vulnerable to inaccuracy caused by human participation. To systematize the process and reduce manual participation, many computer-aided systems have been developed to accomplish leukocyte segmentation and categorization from peripheral blood smear pictures. This study highlights the benefits and drawbacks of several segmentation and classification methods for leukocytes offered by researchers. It also discusses the potential for future research in this area [9].

III. Proposed Methodology

The majority of known approaches rely solely on segmented for WBCs cell counts employing connected component labelling. For segmenting the cytoplasm and nucleus of WBCs, a Gram Schmidt orthogonalization method was combined with the snake methodology, which includes five groups of WBCs

in the blood cell pictures. Following that, a set of attributes was retrieved, along with the local binary pattern and the co-occurrence matrix . In order to improve efficiency, the sequential forward technique was used for selecting features. The suggested method is based on comparing the differences between basophils and eosinophils' colour scatter plot, sizes, and shapes prior carrying out the segmentation technique owing to their dissimilar properties. As a result, the categorization reversible system, a cascaded system using a classification-based segmentation(CSRS) method, was presented.

The following significant challenges face the computer-aided recognizing & counting method in microscopy periphery blood smears:

- The absence of a specific and effective segmentation strategy for various types of WBCs, and
- The complexity of the classification phase brought on by the background's existence makes the retrieved characteristics noisier.

Thus, by establishing a unified comprehensive methodological framework, they hope to solve these two key issues. A initial feature extraction was used in the first phase prior to actually utilising an exact reverse of the sequence of conventional CAD systems by applying the very first classification process before a second segmentation task in the phase 2. This was done because each type of WBC requires unique settings and colour space for accurate segmentation. As a consequence, for precise separation of the two classes, a preparatory categorization procedure (SP1) for performing CP1 was proposed. In order to identify the colour plane at which the initial ROI, known as ROIi, is distinguishable from the background, researchers looked at various pictures of both kinds basophils and eosinophils in each colour space, namely the red, green, and blue (RGB), the hue, saturation, and significance (HSV), the CIELAB, and the YCbCr. The ROIi's brightness range in each particular colour plane was then identified in order to obtain histogram-based characteristics. Then, min-max feature normalisation was used to normalise these characteristics. The supervised infinite feature selection technique is used sequentially during ranking. The information gain, mean of the standardised green plane histogram at the range, and bin location of the highest highpoint at the sub-histogram were thus chosen as characteristics. The cubic SVM is then used to conduct CP1 with these three features as its input. The ROIi for each type is used as an input rather than the actual picture in phase 2, which follows the usual steps of the CAD systems. For combining the basophils and eosinophils images, a wavelet thresholding-based segmentation method (SP2, or "second segmentation process") was suggested. This segmented procedure was predicated on picking the appropriate colour region for each kind and modifying the underlying segmentation technique parameter settings as continues to follow. The suggested bidirectional categorization sub-system 1 is represented by both CP1 and SP2. The final classification step, CP2, is then carried out using the retrieved feature set from SP2. Additionally, subsystem 2 receives data from ROIf to count the WBCs. The suggested unique CSRS computer-aided recognition and counting system framework of basophils and eosinophils cells in microscopic peripheral blood smear pictures is made up of these two subsystems.

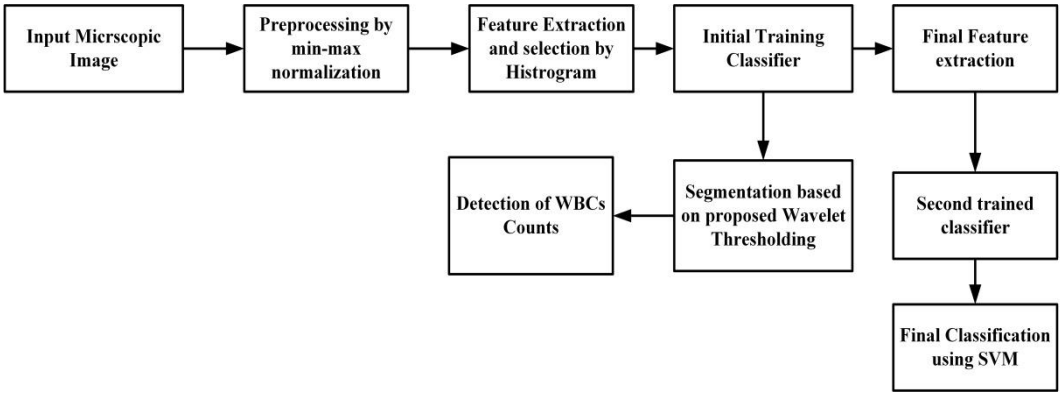

Figure 1. Flow diagram of Proposed CSRS

3.1 Data collection

By using conventional Matlab matrix rules, the database image is stored as a matrix. Indexed images, intensity pictures, binary images, RGB images, and 8-bit images are the five fundamental forms of images that Matlab supports. Images are treated as matrices in MATLAB. This entails dissecting each visual pixel into a matrix's component parts. The generated image matrices for colour and grayscale images varied slightly because MATLAB distinguishes between them. A colour is made up of a few fundamental colours. Consequently, MATLAB divides individual pixel of a colour image referred known as "true colour" into Red, Green, and Blue values. Three matrices—one for each color—represent the full image as a result. A three-dimensional m by n by 3 matrix is created when the three matrices are layered one on top of the other. A grayscale image consists primarily of the hues black and white. These hues, or shades as some may refer to them, are not made up of the

hues Red, Green, or Blue. Instead, they feature a range of colour shades between white and black. Therefore, just one colour channel is required to depict this one range. So, all we need is a 2-dimensional matrix with dimensions m by n by 1. Because the values of such a matrix indicate intensities of a single colour, MATLAB refers to this form of matrix as an intensity matrix. The resulting matrix for a grayscale image with a height of 5 pixels and a width of 10 pixels would be a 5 by 10 matrix.

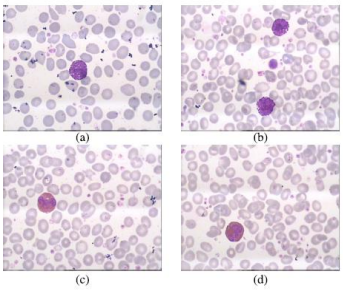

Figure 1. Sample images from the dataset

3.2 Pre-Processing

Pre-processing is necessary for the suggested framework in order to improve photos and obtain finer details by removing noise and using normalising techniques. Pre-processing enhances the structural features, contrast, and brightness of photographs. It significantly increases the visual illustration and produces colourized medical photos with the better overall quality. Pre-processing entails several processes for a gray-scale medical image. Images are typically shown at a resolution of 256 x 256 pixels. The image has been stripped of all text. By employing a weighted average filter, noise is removed. The original image is convolved using a weighted kernel of size 3*3. A sliding kernel of size m n is centred at *(x,y)* in the input images *(x,y)*, where m, n = 3. Consider that zj stands for the processed pixel, with j being the number of pixels below 9. *Rxy* refers to the area where the average of the source image was calculated *(x,y).* In order to correct the dynamic range and highlight an image's details, noise is eliminated from the source and subjected to additional processing. After concluding the noise deportation process, the contrast is increased to draw attention to the picture's minute details. I(x,y) is the sum of the fraction of the pixel under process *zi* and the total number of pixels.

$$I(x,y) = \sum_{i=0}^{n} \frac{z_i}{Total\ Pixels} \tag{1}$$

After the comparison improvement, the image is moved on to the edge enhancement phase. The Sobel edge detector is used for edge detection. The Sobel kernel locates the gradient in the image's vertical and horizontal axes. To determine the size and orientation of edges, slopes are utilised. Here are some Sobel kernel and operation mathematical equations. The variants Kernelx and Kernely, which are horizontal and vertical, are provided in Eqn 2.

$$Kernel_x = \begin{vmatrix} -1 & -2 & -1 \\ 0 & 0 & 0 \\ +1 & +2 & +1 \end{vmatrix}, Kernel_y = \begin{vmatrix} -1 & 0 & +1 \\ -2 & 0 & +2 \\ -1 & 0 & +1 \end{vmatrix}$$
$$Image_x = Kernel_x * Image(x,y), \quad Image_y = Kernel_y * Image(x,y) \tag{2}$$

By combining and separating these derivatives close to the margins, data is improved across edges. In Eqn 2, convolution is calculated using the original image to produce two images with approximate lateral and vertical derivatives. They are employed to determine the gradient of the image, which is depicted in Eqn 3.

$$Image'(x,y) = Image\ \frac{2}{x} + Image\ \frac{2}{y} \tag{3}$$

The resultant image is more informative than the input because the edge intensity has increased noticeably. The image is processed further using the negative transformation. Suppose that the maximum intensity of the image is M. The negative of the image is given in Eqn 4.

$$Image''(x,y) = M - Image'(x,y) \tag{4}$$

3.3 Wavelet based Segmentation

The suggested CSRS fine-tunes the segmentation procedure by utilising the inherent qualities of the WBC pictures. The basophils and eosinophils are used as case studies in this work, and the major goal is to provide

customised different algorithms for each type of microscopy sample. These methods are suggested based on the first categorization CP1 prediction. Thus, the training phase and the testing phase are the two key phases of the suggested system's execution.

- choose the most important colour space after examining the various colour spaces and computing the proposed histogram-based object to background disparity measure to establish the position;
- utilizing the distribution divisions that correspond to its sub-top histogram's and bottom borders, segment the original microscopic picture to discover ROIi;
- removing and selecting the most distinguishable histogram-based features from ROIi to be used in the first classification step CP1; and optimise performance, train the CP1 and CP2 classification systems to set their hyperparameters.

During training, the segmented ROIf's histogram-based properties are fed into the CP2. The proposed classification-segmentation reversible system for classifying and quantifying WBCs is depicted in Fig. 1. In order to appropriately classify the WBC category that use the characteristics that have been obtained from the ROIi, the preliminary classifications procedure' objective was to assign every class to the appropriate segmentation methodology. The second classifier would effectively deliver the final classification result based on the features obtained from the segmented ROIf by using CP2. The initial trained classifier chooses the subsequent segmentation technique during testing based on the classification choice made using the retrieved feature extraction from ROIi. To aid the hematologist's diagnosis, the number of WBCs in the segmented image was then counted. The second trained classifier use CP2 to successfully determine the categorization of the inputs White blood cells by utilising the information that ROIf has gathered.

Algorithm Proposed Wavelet-Based Segmentation
Input: The predicted WBC images$Y = [Y(1), \ldots\ldots, Y(t)]$
Output : $S = [s(1), \ldots, s(t)], n = [n(1), \ldots, n(t)]$
Step 1: For $p \leftarrow 1\ to\ t\ \ do$
Step 2: Convert the $y(p)$ RGB image into LAB colour space to get the L coloured layer.
Step 3: Use PCA to get the rating of the pixels in the L chromatic plane..
Step 4: From the grayscale pixels, extract the scaled PCA score values. scaling the pixels in the grayscale to be between 0 and 1, the scaled grayscale image g_s is created.
Step 5: To acquire the four wavelet coefficients, do a single-level discrete 2-D wavelet decomposition on the GS using a biorthogonal wavelet.
Step 6: In each of the 4 wavelets, determine the threshold and determine the desired threshold. $t_f = \frac{(t_a + t_b + t_h + t_d)}{d_v}\ \ where\ d_v = 2$
Step 7: To acquire d, utilise the inverse discrete 2-D wavelet transform on a single level. To create a binary image, quantize d using the final threshold t_f.
Step 8: Use the 8-bit interconnectivity neighbourhood to conceal the light structures associated to the edges of the binary image. Find the area of the related regions and omit any areas smaller than 500. the segmented masks must be obtained $s(p)$
Step 9: To determine the number of segmented WBCs, tally the linked regions.($nE(q)$).
Step 10: End for , Find S and N

3.4 Extraction of Features using Histograms

Based on examining the ROIi including both classes at the signal path, it was discovered that the ROIi lies between the intensity levels of $\alpha 1 = 0{:}2\ and\ \alpha 2 = 0{:}6$, or between 1 and 2. As a result, data about the grey level distribution of the $ROIi$ sub-histogram within this range (between 2 and 2) was extracted using the histogram-based features. As a result, seven first statistics—average, variation, skewness, kurtosis, energy, and entropy—were employed in addition to the HOBD calculation's indicated bin position for the sub histogram's highest peak. The probabilistic densities of the levels of intensity, which is determined as the proportion of pixels at each intensity level to all pixels within the ROIi, was a determinant of these statistics. The probability density function's definition, found in Eqn 5, were used to get the mean.

$$M = \sum_{\delta=0}^{N_L-1} \rho(\partial)\,.\,\partial \qquad (5)$$

Where ρ(∂) is the total number of possible intensity levels and (δ) is the probability density of the intensity levels' occurrence such that0 ≤ ∂ ≤ Nl - 1 . The variance, skewness, and kurtosis are represented by the central moments k at k D 2; 3; and 4, respectively, which were obtained using Eqn 6.

$$\mu_k = \sum_{\delta=0}^{N_L-1}(\partial - Mx)^k) \ .\partial \tag{6}$$

In this case, the variance represents the intensity level's divergence from the mean, the skewness the degree of the sub-asymmetry histogram's around the mean, and the kurtosis the sharpness of the distribution of intensity levels in comparison to a normal distribution. Even so, Eqn 7's description of the intensity level distribution can be used to determine the homogeneity of the energy.

$$Energy = \sum_{\lambda}(\rho(\partial))^2 \tag{7}$$

While smooth distributions have low entropy values, which may be calculated using the method below in eqn 8, the entropy evaluates the distribution's randomness.

$$Entropy = -\sum_{\delta}\rho(\partial).\log(\rho(\partial)) \tag{8}$$

Additionally, the proposed formula 9 was used to determine the recommended bin location of the greatest peak at the ROIi sub-histogram. Even though the recovered feature vector only has seven features and is low-dimensional, the best feature combination selection necessitates the deletion of irrelevant and noisy features in order to improve the performance of the classification CP1 algorithm. As a result, the most important features were chosen via feature selection to be used in CP1.

$$\alpha_{max} = b\big(\max\big(p(x)\big)\big) \tag{9}$$

3.5 Infinite Feature Selection Under Supervision

Even though there are just seven features in the retrieved feature vector that were calculated from the ROIi, these features may be noisy or useless. A attribute selection approach was used as a result, with the goal of selecting informative features while removing unnecessary and redundant ones.The infinite feature selection filtration approach was selected due to its versatility and independence from the contemporary data, notably in the cases of noise, interclass overlap, and imbalanced classes. A balanced unconstrained densely integrated graph was initially built, in which the nodes stand in for the features and the edges for the connections among these. For each feature pair $(fm;\ fn)$, the adjacency matrix $AJ\ (fm;\ fn)$ of the graph was created to indicate the relevance of both characteristics and their suitability to be chosen as strong candidates. The adjacency matrix for a feature pair is then provided by

$$A_J(f_m, f_n) = S_m.S_n \tag{10}$$

In addition, a path of distance d was made between the nodes of the characteristics fm and fn, passing via generalized nodes whose number is lower than the maximum number of the offered attributes. Additionally, a number of pathways each of extent l can connect the structures fm and fn. The single feature assessment score along a particular path l can be derived by

$$c_l(m) = \sum_{n\in V_N} R_l(m,n) = \sum_{n\in V_N} A_j^l(m,n) \tag{11}$$

here V_N is the node set that represents the specified characteristics and Rl is the total contribution of all feasible l-length pathways. The value of cl directly proportionally reflects the importance of a candidate characteristic. The path length was extended to infinity in order to lessen the computational complexity. In order to prevent the divergence brought on by adding infinite $\boldsymbol{Alj}$ **terms as c(m) D P1 lD1 cl,** the regularisation parameter was added (m). The ultimate ranking scores for each feature, or $cQ(m)$, can then be calculated by

$$c(\tilde{m}) = \big[\tilde{C}e\big]m \tag{12}$$
$$\tilde{C} = (I - rA_J)^{-1} - I$$

where *I* denotes the distance matrix, r is the regularisation parameter, and *e* is a 1-dimensional vector of ones. The characteristic extraction's component values are encoded in the matrices CQ.

3.6 Classification using support vector machine

The Support Vector Machine is a supervised learning technique that looks at the input information for both categorization or estimation tasks using the associated supervised learning. The SVM's learning stage goal is to find the optimum hyper-plane "determination margin" that provides the optimum division between the input classes. Depending on the location of the supplied database in relation to the result boundary, it makes the classification choice during the testing phase. The measured values are typically not linearly distinguishable. The SVM approach converts characteristic vectors from wide variations vectors to identify non - linearly distinguishable datasets. Utilizing the high-dimensional vectors, the SVM was trained. However, this method's main disadvantage is its impacting the overall and time requirement, especially when working with a large dataset. The kernel function approach is then employed as a result [37]. The SVM approach was used in this

study as the primary categorization at CP1 and CP2, which stand for the first and secondary classification procedures, correspondingly. The best hyper-plane for the provided non-linear data was also studied using a number of polynomials and Gaussian kernels. A 5-fold cross-validation resampling technique, for instance, has been used to assess the effectiveness of a framework. The suggested backward classification-segmentation sub-initial system's phase was this CP1. The suggested reversed classification-segmentation sub-system to locate ROIf is based on the first classification performance, and every variety of WBC has distinct properties that call for special adjustments in the final classification SP2 [10].

IV. Result And Discussion

In both sections of the dataset, the suggested technique averaged segmentation accuracy rates of 96.95 percent, 96.8 percent sensitivity, 95.5 percent specificity, and 96. percent F-measure. The suggested methods required 1.2 seconds to segment the photos in the ALL-IDB2 database utilizing an Intel Core i5 machine with 8 GB RAM, whereas they took 4.5 seconds for the images in the ALL-IDB1 dataset. On the other hand, our suggested solution outperformed other cutting-edge approaches on the ALL-IDB database. developed an adaptive technique based on image enhancement that segmented white blood cells with 92 percent accuracy. Combining colour analysis from several colour spaces, with Otsu thresholding, morphology filtration, and key - point labelling for the purpose of identifying White cells. Their findings demonstrated that the S element of the HSV colour space had the greatest segmentation performance, which was 96.92 percent[11]. Suggested a weighted cross-entropy gradient descent for deep learning utilising U-Net for the WBC segmentation using ALL-IDB1, which achieved 94.92 percent segmentation results without data pre-processing[12]. Additionally, achieved a counting accuracy of 98.7 percent utilising the whole ALL-IDB dataset, which is 12.7 percent better than the precision achieved when WBC detection was accomplished via chromaticity conversion and the Hough transform. To increase the accuracy of our counting, additional research on cell overlapping is required. The detailed assessment into the failed instances is also strongly advised for enhancing the effectiveness of the suggested solution. Moreover, an expansion of this study might entail creating deep learning-based methods to lessen the aforementioned restrictions and downsides.

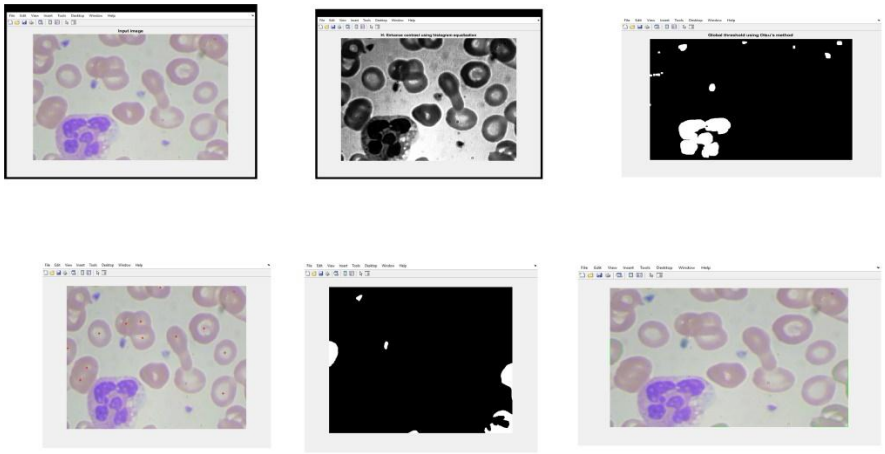

Figure 2. The above figure shows the input images , enhanced contrast using histogram equalization and Global thresholding using Otsu's method and output images of the blood cells.

V. Conclusion

White blood cell characterization, enumeration, and computerized identification of Microscopy imaging in periphery blood cells can be very helpful in making a variety of blood diseases diagnosesThe fundamental differences between the various types of WBCs do, though, tend to make the categorization process more challenging and also have an effect on its reliability. The basophil and eosinophil were employed in this work as case studies prior to constructing the final segmentation method for each category. In order to execute a preliminary categorization technique, these versions were used. The green RGB colour plane was thus identified to be the best colour plane for carrying out an initial ROI identification by the suggested HOBD measure. The preliminary classification technique produced a 93.4 per cent classification performance utilising the 3rd parametric SVM after utilizing the earlier segregated WBC-based greenish flow segmentation method features. The proposed cascaded segmentation and segmentation system was designed to offer a customised wavelet transform-based segmented procedure for every one of the classes. The segmentation technique showed a greater similarity measure of 95.9 per cent for basophils and 96.1 per cent for eosinophils for the same database compared to the latest advancements, which reached a similarity measure of 97.70 per cent for basophils and 95.22 per cent for eosinophils. Furthermore, both classes had median tallying precision of 98.4 per cent.

Following the use of the CSRS depending on the total segmentation outcomes, a 2nd phase categorization was conducted, which achieved a 6.4% improvement in accuracy compared to the earlier classification phase. The suggested framework can also be used in many image processing applications, including telehealth and distant surveillance systems, due to its reliability and precision.

References

[1]. N. M. Karabacak *et al.*, "Microfluidic, marker-free isolation of circulating tumor cells from blood samples," *Nat. Protoc.*, vol. 9, no. 3, pp. 694–710, Mar. 2014, doi: 10.1038/nprot.2014.044.

[2]. Z. Yang *et al.*, "Comparisons of neutrophil-, monocyte-, eosinophil-, and basophil- lymphocyte ratios among various systemic autoimmune rheumatic diseases," *APMIS*, vol. 125, no. 10, pp. 863–871, Oct. 2017, doi: 10.1111/apm.12722.

[3]. J. Chung, X. Ou, R. P. Kulkarni, and C. Yang, "Counting White Blood Cells from a Blood Smear Using Fourier Ptychographic Microscopy," *PLOS ONE*, vol. 10, no. 7, p. e0133489, Jul. 2015, doi: 10.1371/journal.pone.0133489.

[4]. M. I. Razzak and B. Alhaqbani, "Automatic Detection of Malarial Parasite Using Microscopic Blood Images," *J. Med. Imaging Health Inform.*, vol. 5, no. 3, pp. 591–598, Jun. 2015, doi: 10.1166/jmihi.2015.1417.

[5]. T. Bergen, D. Steckhan, T. Wittenberg, and T. Zerfass, "Segmentation of leukocytes and erythrocytes in blood smear images," in *2008 30th Annual International Conference of the IEEE Engineering in Medicine and Biology Society*, Vancouver, BC, Canada, Aug. 2008, pp. 3075–3078. doi: 10.1109/IEMBS.2008.4649853.

[6]. L. Kass, G. Harrison, and C. Lindheimer, "A new stain for identi cation of avian leukocytes," p. 6.

[7]. M. Yu, S. Stott, M. Toner, S. Maheswaran, and D. A. Haber, "Circulating tumor cells: approaches to isolation and characterization," *J. Cell Biol.*, vol. 192, no. 3, pp. 373–382, Feb. 2011, doi: 10.1083/jcb.201010021.

[8]. A. Loddo, L. Putzu, C. Di Ruberto, and G. Fenu, "A Computer-Aided System for Differential Count from Peripheral Blood Cell Images," in *2016 12th International Conference on Signal-Image Technology & Internet-Based Systems (SITIS)*, Naples, 2016, pp. 112–118. doi: 10.1109/SITIS.2016.26.

[9]. S. Sapna and A. Renuka, "Techniques for Segmentation and Classification of Leukocytes in Blood Smear Images - A Review," in *2017 IEEE International Conference on Computational Intelligence and Computing Research (ICCIC)*, Coimbatore, Dec. 2017, pp. 1–5. doi: 10.1109/ICCIC.2017.8524465.

[10]. A. Zien, G. Ratsch, S. Mika, B. Scholkopf, T. Lengauer, and K.-R. Muller, "Engineering support vector machine kernels that recognize translation initiation sites," *Bioinformatics*, vol. 16, no. 9, pp. 799–807, Sep. 2000, doi: 10.1093/bioinformatics/16.9.799.

[11]. H. Li, X. Zhao, A. Su, H. Zhang, J. Liu, and G. Gu, "Color Space Transformation and Multi-Class Weighted Loss for Adhesive White Blood Cell Segmentation," *IEEE Access*, vol. 8, pp. 24808–24818, 2020, doi: 10.1109/ACCESS.2020.2970485.

[12]. N. H. Mahmood, P. C. Lim, S. M. Mazalan, and M. A. A. Razak, "BLOOD CELLS EXTRACTION USING COLOR BASED SEGMENTATION TECHNIQUE," *Pharm Res*, p. 10, 2013.